Northumbria Research Link

Citation: Zhang, Zhichao, Kouris, Georgios D., Kouris, Panos D., Hensen, Emiel J. M., Boot, Michael D. and Wu, Dawei (2021) Investigation of the combustion and emissions of lignin-derived aromatic oxygenates in a marine diesel engine. Biofuels, Bioproducts and Biorefining, 15 (6). pp. 1709-1724. ISSN 1932-104X

Published by: Wiley-Blackwell

URL: https://doi.org/10.1002/bbb.2267 <https://doi.org/10.1002/bbb.2267>

This version was downloaded from Northumbria Research Link: http://nrl.northumbria.ac.uk/id/eprint/46698/

Northumbria University has developed Northumbria Research Link (NRL) to enable users to access the University's research output. Copyright © and moral rights for items on NRL are retained by the individual author(s) and/or other copyright owners. Single copies of full items can be reproduced, displayed or performed, and given to third parties in any format or medium for personal research or study, educational, or not-for-profit purposes without prior permission or charge, provided the authors, title and full bibliographic details are given, as well as a hyperlink and/or URL to the original metadata page. The content must not be changed in any way. Full items must not be sold commercially in any format or medium without formal permission of the copyright holder. The full policy is available online: http://nrl.northumbria.ac.uk/policies.html

This document may differ from the final, published version of the research and has been made available online in accordance with publisher policies. To read and/or cite from the published version of the research, please visit the publisher's website (a subscription may be required.)

Northumbria University NEWCASTLE

University Library

Original Article

Biofpr Biofuels Bioproducts & Biorefining

Investigation of the combustion and emissions of lignin-derived aromatic oxygenates in a marine diesel engine

Zhichao Zhang, Department of Mechanical and Construction Engineering, Faculty of Engineering and Environment, Northumbria University, Newcastle upon Tyne, UK
Georgios D Kouris, School of Engineering, Newcastle University, Newcastle upon Tyne, UK
Panos D Kouris, Emiel J M Hensen, Laboratory of Inorganic Materials and Catalysis, Department of Chemical Engineering and Chemistry, Eindhoven University of Technology, Eindhoven, The Netherlands
Michael D Boot, Laboratory of Inorganic Materials and Catalysis, Department of Chemical Engineering and Chemistry, Eindhoven University of Technology, Eindhoven, The Netherlands; Energy Technology, Department of Mechanical Engineering, Eindhoven University of Technology, Eindhoven, The Netherlands
Dawei Wu, Department of Mechanical Engineering, School of Engineering, University of Birmingham, Birmingham, UK

Received April 25 2021; Revised June 09 2021; Accepted June 21 2021;
View online at Wiley Online Library (wileyonlinelibrary.com);
DOI: 10.1002/bbb.2267; *Biofuels, Bioprod. Bioref.* (2021)

Abstract: As a hard-to-decarbonize sector, the shipping industry is experiencing demands to accelerate the transition from fossil fuels to alternative low-carbon fuels, to significantly reduce the negative impacts on the environment. Biofuels are regarded as one of the solutions for decarbonization in the marine sector. This paper introduces a lignin-derived drop-in biofuel, 2-methoxy-4-propylphenol (2M4PP), from non-edible feedstocks and investigates engine performance using its 10% (by volume) blend with standard diesel fuel (DF) at variable engine speeds and loads. Results show insignificant difference between the in-cylinder pressures of the proposed blend and DF. The diesel-2M4PP blend emits less carbon monoxide (CO) and nitric oxide (NO_x) than DF at all speeds by up to 39.6% and 10.7% respectively, although its brake-specific fuel consumption (BSFC) is higher. A Ricardo wave model, which is validated with engine experimental data at 2400 rpm speed and full load, is investigated by adjusting injection pressure, injection timing, injection duration and nozzle diameter. The optimal parameters, i.e., 214 bar injection pressure, 6° injection timing, 41.4° injection duration, and 0.37 mm injector orifice, lead to the best engine performance with improved brake power, reduced NO_x emissions, and limited influence on BSFC and hydrocarbon emissions compared to DF. © 2021 The Authors. *Biofuels, Bioproducts and Biorefining* published by Society of Industrial Chemistry and John Wiley & Sons Ltd

Key words: lignin; biofuel; drop-in fuel; marine engine

Correspondence to: D Wu, Department of Mechanical Engineering, School of Engineering, University of Birmingham, Birmingham B15 2TT, UK. E-mail: d.wu.1@bham.ac.uk

SCI where science meets business

© 2021 The Authors. *Biofuels, Bioproducts and Biorefining* published by Society of Chemical Industry and John Wiley & Sons, Ltd.
This is an open access article under the terms of the Creative Commons Attribution License, which permits use, distribution and reproduction in any medium, provided the original work is properly cited.

Introduction

According to recent research, over 70% of global trade is being carried on board ships burning fossil fuels.[1] Due to the environmental impact and the increasing demand for shipping, the International Maritime Organization (IMO) published regulations including the International Convention for the Prevention of Pollution from Ships (MARPOL) Annex VI to reduce NO_x, sulfur oxide $(SO)_x$, and Particulate Matters (PM).[2,3] Developing renewable fuel technologies is one viable solution to tackle the emissions issues in the marine sector.

Biofuel is a low-carbon renewable energy source with much lower life-cycle greenhouse gas (GHG) emissions and other pollutant emissions compared with the emissions from fossil fuels used in diesel engines.[4] Many studies have been conducted on engine performance of various first-generation biofuels, which are derived from edible feedstocks. Jeon and Park[5] studied the biodiesel derived from soybean in a single-cylinder diesel engine at a fixed load and speed, and found that soot emitted by biodiesel was at a lower level than that from diesel fuel (DF). Özener *et al.*[6] conducted experiments on biodiesel converted from soybean oil and its blends with diesel fuel in a single-cylinder direct-injection diesel engine at varying speed. The results demonstrated decreased CO but increased NO_x emissions. In contrast, Shen *et al.*[4] investigated the performance of waste cooking oil-derived biodiesel blends on trucks driven by diesel engines. It was found that the total fuel consumption did not show a clear decreasing trend when the engine burns the biodiesel blends, and both CO and NO_x emissions decreased with increasing biodiesel content. The study demonstrated an actual application, but the influence of engine speed and load was not identified. Nabi *et al.*[7] conducted engine experiments with both varying speed and load on waste cooking oil, and demonstrated that the engine fueled with biodiesel had slightly lower power, higher BSFC, less emissions of CO, hydrocarbons (HC), and PM, although higher NO_x was recorded. The studies on the first-generation biofuels showed some inconsistency in the results of NO_x emissions when they were compared with DF. The 'food versus fuel' debate caused by the first-generation biofuels derived from edible sources hinders a wide uptake of biofuels in many developing countries.

Second-generation biofuels are generally produced from lignocellulosic biomass, which comprises non-edible feedstocks, in contrast to feedstocks used for first-generation biofuels.[8] Lignocellulosic biomass represents an abundant renewable carbon source for biofuels as its overall weight on the Earth is estimated to be $(1.85 \sim 2.4) \times 10^{12}$ tons, while $(1.5 \sim 1.8) \times 10^{11}$ tons of photosynthesis biomass is produced every year.[9] Until recently, mainly cellulose in lignocellulosic biomass (30–50%) was used for second-generation biofuel production (e.g., ethanol), whereas lignin in lignocellulosic biomass (10–20%) is increasingly recognized as an additional valuable resource for biofuel production.[10] The total lignin availability in the biosphere exceeds 300 billion tonnes and increases by around 20 billion tonnes annually.[9] The chemical pulping industry generates up to 70 million tonnes of lignin biowaste annually, and the emerging cellulosic ethanol production may generate a comparable amount of lignin biowaste in the future.

Lignin is a non-edible, high-aromatic, complex three-dimensional polymer biomass, which has the potential to be converted to biofuels for diesel engine applications. Sun *et al.*[11] produced ammoniated lignin diesel from papermaking black liquor, and demonstrated that the ammoniated lignin diesel has high stability and small smoke intensity when used in blends with DF on a diesel engine. Lignin has a complex poly-aromatic molecular structure; therefore, it has to be depolymerized into useful monomeric aromatics before being blended with DF. As aromatic oxygenates blended with hydrocarbon fuels demonstrated their ability to suppress NO_x and soot emissions from diesel engines,[12] researchers extracted them from lignin and tested them as drop-in biofuels. Tian *et al.*[13] investigated the engine performance of several biofuels including three types of lignin-derived aromatic oxygenates with low toxicity, and found they improved knock resistance and fuel economy. Zhou *et al.*[8,14] derived another two substances, i.e., 2-phenyl ethanol, and cyclohexane ethanol, from lignin, and studied their performance on a heavy-duty diesel engine. The results indicated that the biofuels have similar fuel consumption as diesel fuel, although 2-phenyl ethanol emitted the largest amount of soot. Kumar *et al.*[15] tested lignin derived cyclohexanol in a diesel engine. In contrast, they claimed that the thermal efficiency and the fuel consumption of the biofuel were worse in comparison with those of DF. Meanwhile, NO_x, CO, and HC were all found increased when using cyclohexanol as the fuel compared with DF. From the existing literature on engines powered with lignin-derived biofuels, the influence of the biofuels on engine performance is controversial due to various engines used in experiments, different operation modes, etc. In the meantime, there are more potential biofuel species derived from lignin yet to be tested and investigated in diesel engines.

In recent years, a strategy (lignin-first process or reductive catalytic fractionation, seen in Fig. 1) towards

© 2021 The Authors. *Biofuels, Bioproducts and Biorefining* published by Society of Chemical Industry and John Wiley & Sons, Ltd.

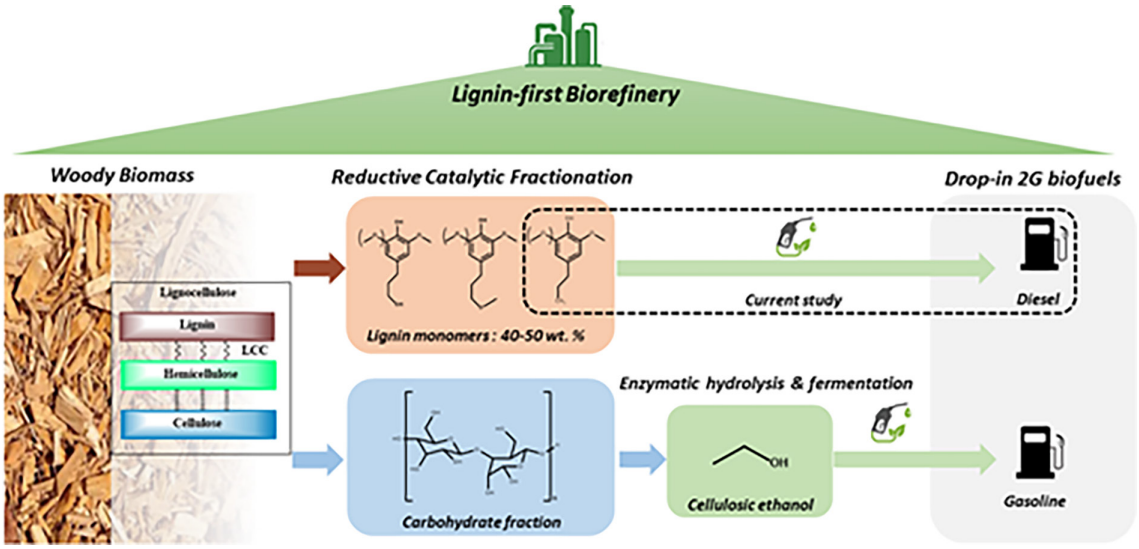

Figure 1. Integrated lignin-first biorefinery concept for production of drop-in biofuels.

lignocellulose upgrading has been advocated that aims to convert native lignin biomass directly upon release from the lignocellulosic matrix very selectively into 2–3 monomers (alkyl-methoxy phenols) in high yields (40–50 wt%).[16–18] Based on the literature,[19] as can be gathered from compression ignition (CI) engine experiments, the overall engine performance generally benefits from the addition of benzenoids that have both a low reactivity (e.g., high cetane number, low octane number) and high energy density per unit of volume. Benchmarked against toluene, arguably the best non-oxygenated benzenoid when it comes to reactivity and energy density, the addition of a single functional oxygen group (e.g., anisole) does not noticeably impact either property. Conversely, the presence of a second oxygen group, e.g., (alkyl) guaiacols, is detrimental for both fuel reactivity and heating value. Accordingly, guaiacols are not ideal for use in engines. Moreover, their yield from technical lignin depolymerization is relatively low. From both yield rate and engine performance perspectives, alkyl phenols such as 4-ethyl phenol and 4-methyl phenol, promise to be superior biofuel candidates, and their selective production via the lignin-first process has been demonstrated by many research groups.[20] A previous study by Kouris *et al.*[21] selected 2M4PP as the model compound derived from lignin and blended it with heptane at 10% content. The results demonstrated that 2M4PP is likely to be a drop-in biofuel to diesel application, as the blend had similar auto-ignition characteristics to diesel fuel. However, the actual performance of 2M4PP blended with diesel fuel is still unknown in a diesel engine.

This paper investigates lignin derived 2M4PP as a drop-in biofuel to be used on a marine diesel engine and identifies the engine performance in terms of in-cylinder pressure, brake power, fuel consumption and pollutant emissions by both experiments and numerical models. The diesel engine in the study is also optimized for burning the 2M4PP and DF blend by configuring its fuel injection parameters using the numerical model.

Process for lignin derived biofuel production

The production of lignin-derived, drop-in biofuels requires lignin depolymerization. The underlying chemistry for lignin depolymerization is the cleavage of lignin interlinkages, particularly the β-O-4 linkage. Most delignification and biomass pre-treatment processes (i.e., Kraft, organosolv, soda, or steam explosion) can break ether bonds. However, the reactive intermediates produced during delignification are prone to form carbon–carbon bonds, resulting in a recondensed and polymeric lignin.

Lignin-first processing is the broadly accepted umbrella term for solvent-based methods in which lignin preservation, together with that of the polysaccharides, is considered upfront, moving away from the current practice of having to deal with an intractable lignin product at the end of a biorefining process. To date, there have been several approaches reported for lignin-first refining; defined as an active stabilization approach that liberates lignin from the plant cell wall and prevents condensation reactions though either catalysis or protection group chemistry.[20] The most common

© 2021 The Authors. *Biofuels, Bioproducts and Biorefining* published by Society of Chemical Industry and John Wiley & Sons, Ltd.

methodology comprises solvent-based lignin extraction from biomass in the presence of a transition metal under a hydrogen atmosphere or with the aid of a hydrogen-donor solvent or another reducing agent.[22] This methodology is generally now termed reductive catalytic fractionation (RCF).

Reductive depolymerization cleaves lignin ether bonds in a hydrogen atmosphere or hydrogen donor solvent and is recognized as a promising method to obtain lignin aromatic monomers with high monomer yield and product selectivity.[23] Depending on the reaction conditions, the products can be oxygenated aromatic monomers, deoxygenated aromatic monomers and ring-hydrogenated aromatics.[24] Reductive depolymerization is targeting the hydrogenolysis of native lignin ether bonds and shows poor performance for carbon–carbon cleavage; technical lignin is therefore not an ideal feedstock due to loss of ether bonds and the formation of recalcitrant carbon–carbon bonds during delignification. In the RCF method, lignin is selectively dissolved in polar organic solvents (i.e., methanol) and then depolymerized into monomers. An important feature of this process is that the unsaturated lignin intermediates can be stabilized simultaneously by catalytic hydrogenation, which is essential to avoid recondensation and obtain a high monomer yield. Sels and co-workers selectively extracted and converted *in planta* birch wood into a high yield of phenolic monomers (52%) under 30 bar H_2 using Ru/C at 250°C for 6 h.[25]

We also reported the use of homogeneous metal triflates to release lignin rapidly from lignocellulosic biomass.[26] Combined with metal catalyzed hydrogenolysis (Pd/C), the process converts biomass into lignin-derived alkylmethoxyphenols (36–48%) and cellulose under mild conditions (180 °C, 2 h). The cellulose-rich residue is ideal feedstock for established biorefining processes (i.e., cellulosic ethanol). It is interesting to note that the product selectivity of the lignin oil can be tuned by specific catalyst choice. For instance, Ru/C typically yields propyl-substituted methoxyphenols, whereas Pd/C can increase the OH content in lignin monomers, resulting in propanol-substituted methoxyphenols.[27] The monomer yield and product selectivity also depend on the type of lignocellulosic feedstock. Depolymerization of hardwood lignin leads to high yields (>40%) of the syringol type of monomer, whereas depolymerization of softwood lignin results in the guaiacol type of monomer with lower yields (<30%).[28]

Overall, lignin oil after the RCF process is mainly composed of the monomeric alkylmethoxyphenols (i.e., 2-methoxy-4-propyl phenol, 2,6-dimethoxy-4-propylphenol), which, after isolation from the product mixture, can be used as feedstock for fuels, chemical or materials.

Methodologies

Fuel formulation

The lignin-derived biofuel in this study is 2-methoxy-4-propyl phenol (2M4PP), and it is obtained from Sigma-Aldrich, UK. The depolymerization process itself is out of the scope of this paper; it assumes that such a catalytic process, most likely will eventually become available on a commercial scale to supply the fuel and chemical industry with highly desired renewable aromatic chemicals. Its molecular structure is shown in Fig. 2. The oxygenate in question is assumed to be of low toxicity for humans given that the US Food and Drug Administration (FDA Part 172, Subpart F) has approved its use as a food additive for direct addition to food for human consumption, where it is typically used as flavorant (e.g., 2-phenyl ethanol = rose).

The 2M4PP is blended with standard DF with a volume fraction of 10%. It is named LD10 for the engine experiment. The mixture is then tested in the experimental system and a numerical model, and DF is also tested as a reference. The main properties of the aromatic oxygenate, and standard diesel fuel are listed in Table 1. The determination of derived cetane number (DCN) of the aromatic oxygenate is derived using the ASTM protocol DIN EN 15195, via the external laboratory ASG Analytic Service (Germany). Boot[32] studied the performance of various types of oxygenates in both compression ignition and spark injection engines, and found that all reviewed aromatic oxygenates shared a low DCN. Moreover, it was found that adding O atoms to aromatic branches will decrease the bond dissociation energy (BDE) of side chain C—H bonds. Oxygenation, though, will hardly affect the BDE of aromatic C—H bonds. The initiation of the auto-ignition chemistry, given the stable benzene base central to all aromatics, typically occurs on the side chains when present. Overall, more or longer chains in aromatic oxygenates will have an acceleratory effect on the overall reaction rate, which makes the selected 2M4PP a good candidate as a drop-in biofuel component.

The experimental system

The experiments are conducted on a Cussons engine test bed P8250 (UK), which consists of a marine diesel engine and an engine control unit as shown in Fig. 3. The engine

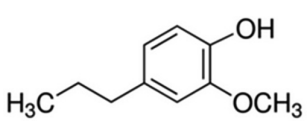

Figure 2. Molecular structure of 2M4PP.

© 2021 The Authors. *Biofuels, Bioproducts and Biorefining* published by Society of Chemical Industry and John Wiley & Sons, Ltd.

Table 1. Main properties of 2M4PP and standard diesel fuel.

Property	2-methoxy-4-propyl phenol	Diesel
Derived cetane number (DCN)*	18	48.66
Lower heating value (MJ kg^{-1})*	31.48	42.85
Density (kg m^{-3})*	1038	762.55
Viscosity (m^2 s^{-1}) at 100°C [32–34]	4.91×10^{-3}	7.13×10^{-4}
C content (wt %)*	66.68	86
H content (wt %)*	8.32	14
O content (wt %)*	24.99	0
N content (wt %)*	0	0
S content (wt %)*	0	
Flash point (°C)[29–31]	113	>52
Boiling point (°C)[29–31]	250	190 ~ 280

*Properties are provided by Eindhoven University of Technology.

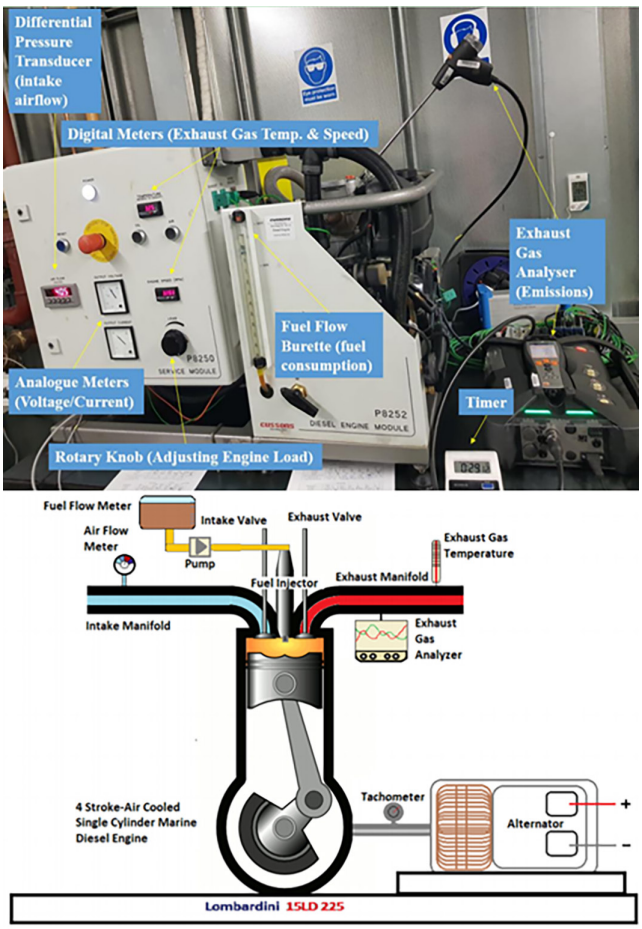

Figure 3. Layout of the engine test bed.

is a four-stroke compression ignition engine, and its specifications are shown in Table 2.

Table 2. Specifications of the 15LD 225 marine diesel engine.

Parameter	Value
Cycle	Four-stroke diesel
Number of cylinders	1
Injection method	Direct injection
Aspiration	Natural
Bore (mm)	69
Stroke (mm)	60
Displacement (cm^3)	224
Compression ratio	21
Max speed (rpm)	3600
Max torque (nm)	10.4 at 2400 rpm
Fuel consumption (g kwh^{-1})	267 at rated power
Oil consumption (L h^{-1})	0.0021
Cylinder head surface (mm^2)	3739.28
Rod length (mm)	100

In the engine control unit, the intake air flow and fuel flow are measured by a differential pressure transducer and a fuel-flow measuring burette, respectively. The engine speed is recorded by a proximity switch mounted on the engine module. The torque is provided by a three-phase alternator, and current (A) and voltage (V) are displayed on two analogue meters. A Kistler 6052C high-temperature pressure sensor from Switzerland is installed to detect the in-cylinder pressure with the accuracy of ±0.5%. The signal is transmitted to a computer via a Kistler 5018A charge amplifier. A K-type thermocouple is placed at the exhaust manifold to detect the exhaust gas temperature, and a UK made Testo 350 exhaust gas analyzer is mounted on the same place to measure the carbon monoxide (ppm), nitric oxide (ppm), carbon dioxide (vol.%), and nitrogen dioxide (ppm). The specifications of the Testo 350 exhaust gas analyzer are listed in Table 3.

The LD10 and DF were used in the engine experiments, which were conducted at full load and various engine speeds. The details are shown in Table 4.

Numerical model

A 1D numerical model is developed with Ricardo WAVE according to the specifications of the experimental engine, as shown in Table 2. In this model, the engine torque, fuel consumption and power as well as emissions including NO_x, CO and HC are validated by experimental data related to LD10 and diesel fuel at 2400 rpm speed and 100% load. Then, the engine optimization is conducted under the same conditions by adjusting injection pressure, different injection

© 2021 The Authors. *Biofuels, Bioproducts and Biorefining* published by Society of Chemical Industry and John Wiley & Sons, Ltd.

Table 3. Specifications of the Testo 350 exhaust gas analyzer.

Parameter	Accuracy	Response time
O_2	±0.2Vol.%	<20 s
CO	±10 ppm (0 ~ 199 ppm)	<40 s
	±5% (200 ~ 2000 ppm)	
	±10% (rest of range)	
NO	±5 ppm (0 ~ 99 ppm)	<30 s
	±5% (100 ~ 1999 ppm)	
	±10% (rest of range)	
NO_2	±5 ppm (0 ~ 99.9 ppm)	<40 s
	±5% (rest of range)	
SO_2	±5 ppm (0…99 ppm)	<30 s
	±5% (100 ~ 1999 ppm)	
	±10% (rest of range)	
H_2S	±2 ppm (0 ~ 39.9 ppm)	<35 s
	±5% (rest of range)	

Table 4. Experimental conditions.

Speed (rpm)	Load (%)
2000	100
2400	100
2800	100
3200	100

timing, different injection duration and nozzle diameter to confirm their best combination when running on LD10.

In the numerical model, the Diesel Wiebe combustion model is employed to describe the rate of fuel mass burned in thermodynamic calculations. It covers the premixed combustion, diffusion combustion, and slow late combustion (tail burning) in the engine cylinder. The burned fuel mass fraction W based on the crank angle can be calculated from Eqn (1):

$$W = p_f\left\{1-\left[1-\left(0.75\tau\right)^2\right]^{5000}\right\}+d_f\left\{1-\left[1-\left(cd_3\tau\right)^{1.75}\right]^{5000}\right\} +t_f\left\{1-\left[1-\left(ct_3\tau\right)^{2.5}\right]^{5000}\right\} \quad (1)$$

where p_f, d_f and t_f are the mass fractions of the premixed, diffusion and tail combustion respectively, and τ is the burn duration term determined by Eqn (2):

$$\tau = \frac{\theta-\theta_b}{125\left(\frac{RPM}{BRPM}\right)^{0.3}} \quad (2)$$

θ and θ_b here refer to the crank angle and the crank angle at the start of combustion respectively, whilst RPM and BRPM are the engine speed and reference speed. The mass fraction of the premixed combustion can be either user input or obtained from the ignition delay model. The mass fractions of the diffusion and tail burn curves are then calculated using Eqns (3) and (4):

$$d_f = \left(1-p_f\right)\left(1-\alpha\right) \quad (3)$$

$$t_f = \left(1-p_f\right)\alpha \quad (4)$$

and α is obtained by:

$$\alpha = 0.6*\left[\min\left(\varnothing, 0.85\right)\right]^2 \quad (5)$$

where $\varnothing$ is the trapped equivalence ratio. cd_3 and ct_3 are the burn duration coefficients for the diffusion and tail combustion, which can be calculated by Eqns (6) and (7):

$$cd_3 = \frac{0.055}{1+0.5\min\left(\varnothing,0.85\right)} \quad (6)$$

$$ct_3 = \frac{3.7cd_3}{1+1.12\min\left(\varnothing,0.85\right)} \quad (7)$$

The ignition delay $\Delta\theta_{delay}$ is determined by the in-cylinder temperature and pressure, as well as the fuel Cetane Number (CN), as illustrated in Eqn (8):

$$\Delta\theta_{delay} = 323exp^{\min\left(\frac{2100C}{T_{sum}},80\right)/P_{sum}} \quad (8)$$

The variables in Eqn (8) are:

$$C = \frac{67}{25+DCN} \quad (9)$$

$$T_{sum} = \sum_n \frac{T_c^n+T_c^0}{2}*\frac{\Delta\theta_n}{\theta_{n+1}-\theta_0} \quad (10)$$

$$P_{sum} = \sum_n \frac{P_c^n+P_c^0}{2}*\frac{\Delta\theta_n}{\theta_{n+1}-\theta_0} \quad (11)$$

where DCN is the derived cetane number, T_c^n and P_c^n are current in-cylinder temperature and pressure respectively, whilst T_c^0 and P_c^0 are the in-cylinder temperature and pressure at the start of injection respectively. Here, $\Delta\theta_n$ refers to the time-step size and θ_0 is the crank angle at the start of injection.

© 2021 The Authors. *Biofuels, Bioproducts and Biorefining* published by Society of Chemical Industry and John Wiley & Sons, Ltd.

The Woschni model is appropriate for the heat transfer on all engine cylinder elements, which assumes a uniform heat flow coefficient and velocity on all cylinder surfaces. Thus, the Woschni heat transfer coefficient is calculated using Eqn (12):

$$h_g = 0.0128 D^{-0.20} P^{0.80} T^{-0.53} v_c^{0.8} C_{enht} \quad (12)$$

where D, P, T, v_c and C_{enht} are the cylinder bore, in-cylinder pressure, in-cylinder temperature, characteristic velocity, and multiplier respectively. For diesel jet combustion, C_{enht} is equal to 1, and v_c is determined by the cylinder geometry and operating condition (e.g., in-cylinder pressure and temperature, indicated mean effective pressure, clearance volume and displacement etc.).

Results and discussion

In this section, the engine performance with LD10 is analyzed at various speeds and constant loads. The engine experimental data are used to validate the Ricardo Wave model, which is then configured to optimize the engine for the use of LD10.

Engine experiments

Figure 4 illustrates the in-cylinder pressure of DF and LD10 at different speeds.

As shown in Fig. 4, both fuels in the tests experience reduction of peak in-cylinder pressure when engine speed increases, which is attributed to less combustion duration at higher speeds. The in-cylinder pressure of LD10 shows small discrepancies compared to that of DF at each engine speed. As the volumetric fraction of 2M4PP is low in LD10, the volumetric energy density of LD10 (32.68 kJ mm^{-3}) is similar to that of DF, due to the larger density of 2M4PP. The lower heating value (LHV) of LD10 (41.36 MJ kg^{-1}) is slightly lower than that of DF. As a result, the amount of heat release during combustion has no significant difference. Consequently, using LD10 as a fuel has minimum impact on the amount of single injection in the testing engine.

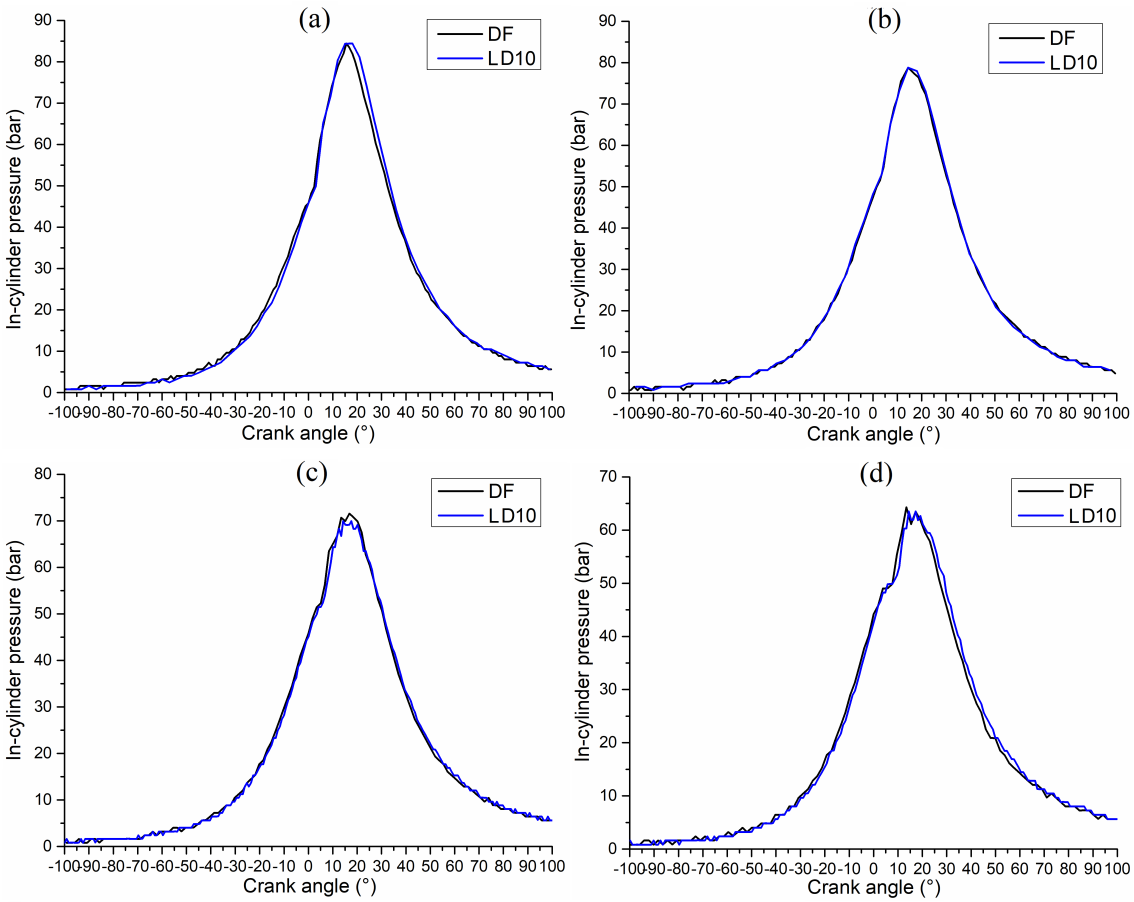

Figure 4. In-cylinder pressure of test fuels at 100% load and 2000 rpm (a), 2400 rpm (b), 2800 rpm (c) and 3200 rpm (d) respectively.

© 2021 The Authors. *Biofuels, Bioproducts and Biorefining* published by Society of Chemical Industry and John Wiley & Sons, Ltd.

The BSFC of both fuels is shown in Fig. 5. LD10 has higher BSFC than DF, due to the higher density of 2M4PP, leading to the higher density of LD10 (790.1 kg m^{-3}).

As illustrated in Fig. 6, the CO emission of LD10 is lower than that of DF by up to 39.6%, despite its slightly higher viscosity. Usually, the higher viscosity of a fuel is harmful to atomization, which may result in incomplete combustion, sequentially easier CO formation. On the other side, the oxygen content of 2M4PP promotes the complete oxidation of carbon in the fuel molecules during combustion, which may reduce CO emissions, as demonstrated in the literature.[6] The reason that CO emission increases at higher speed for both fuels is attributed to more fuel consumption.

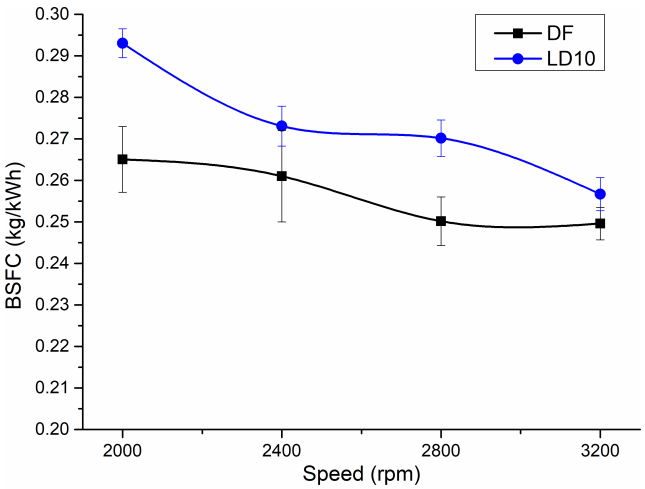

Figure 5. Brake specific fuel consumption of both fuels in 100% load of different engine speeds.

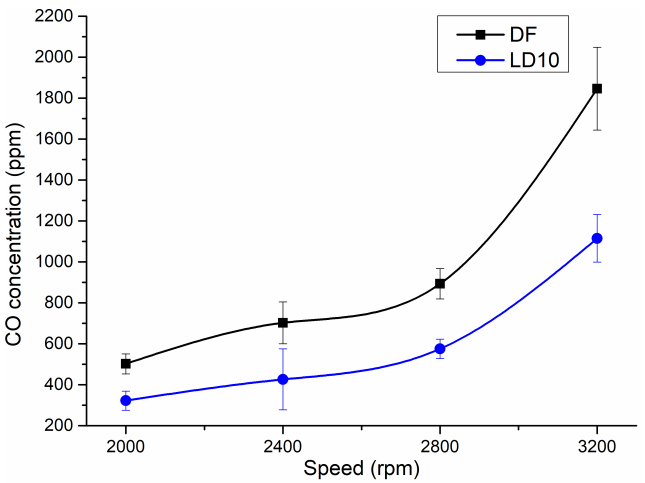

Figure 6. CO emissions of both fuels at varying speeds and 100% load.

In terms of NO_x, LD10 emits less than DF, as illustrated in Fig. 7. According to the literature,[33,34] NO is the dominant composition of NO_x emissions, and is mainly formed through the thermal NO mechanism in high-temperature and lean-burning zones. The majority of NO_x emission is produced during combustion, so it is sensitive to combustion temperature. Due to the slightly lower LHV of LD10, its combustion temperature is relatively lower than that of DF, which may contribute to lower NO_x. As a result, the deduction of NO_x is more significant at 3200 rpm in terms of its percentage reduction (about 10.7%). Figure 7 also indicates that NO_x emissions of LD10 and DF both drop with increasing engine speed caused by decreasing residence time for NO_x formation.

Model validation

The experimental data for LD10 and DF obtained at 2400 rpm and full load on the testing engine are employed to validate the numerical models in Ricardo WAVE. The numerical models are configured and run under the same engine conditions as the experiments. The in-cylinder pressures of both fuels obtained by the numerical models are shown in Fig. 8.

As shown in Fig. 8, the curves of in-cylinder pressure of DF and LD10 from the numerical models agree with the experimental data well at most crank angles. The errors are within 2.4% and 2.2%, respectively, at the peak pressures, which means the models have excellent credibility to predict engine in-cylinder pressures with either DF or LD10 used as a fuel. As a result, the brake powers predicted by the models are in good alignment with the experimental data, as shown in Fig. 9.

Figure 10 illustrates the BSFC of both fuels. For DF and LD10, BSFCs obtained by the numerical models are close to

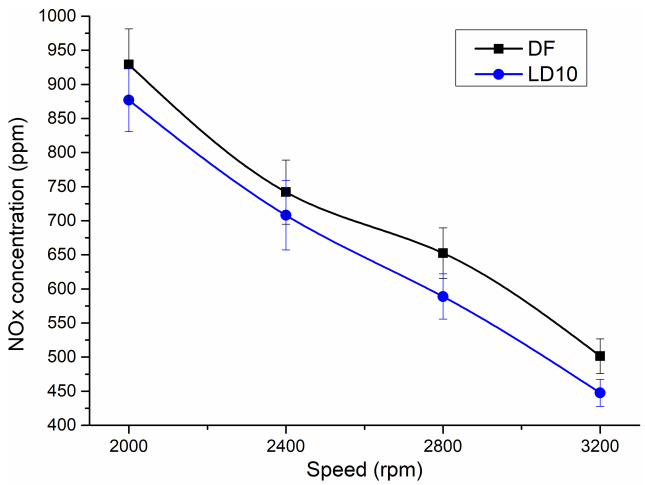

Figure 7. NO_x emissions of both fuels at varying speeds and 100% load.

© 2021 The Authors. *Biofuels, Bioproducts and Biorefining* published by Society of Chemical Industry and John Wiley & Sons, Ltd.

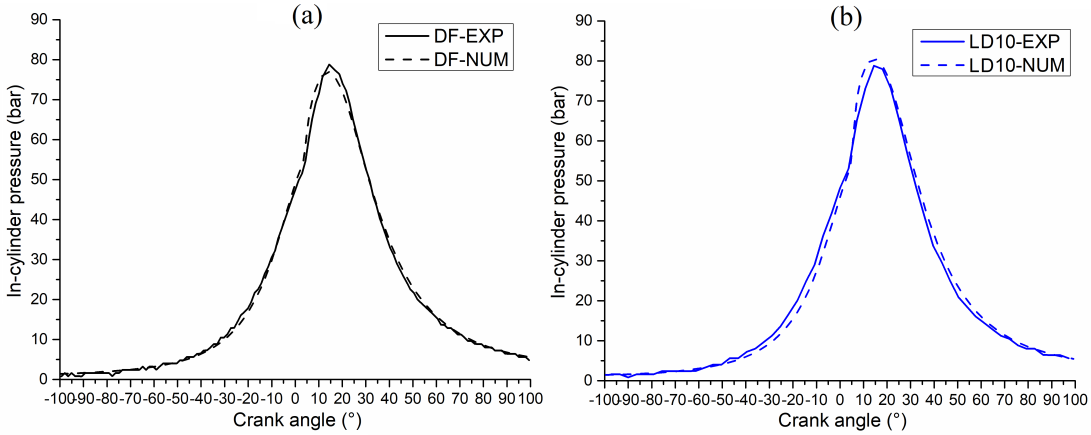

Figure 8. Comparison of in-cylinder pressure of DF (a) and LD10 (b) at 2400 rpm and full load between experiments and numerical models.

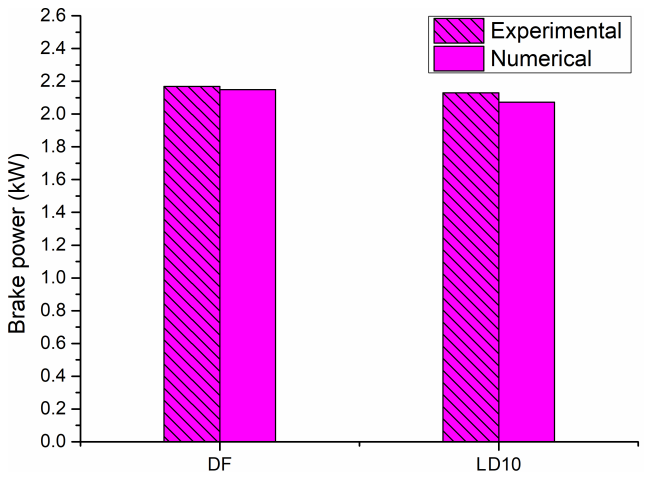

Figure 9. Comparison of brake power at 2400 rpm and full load between experimental and numerical results.

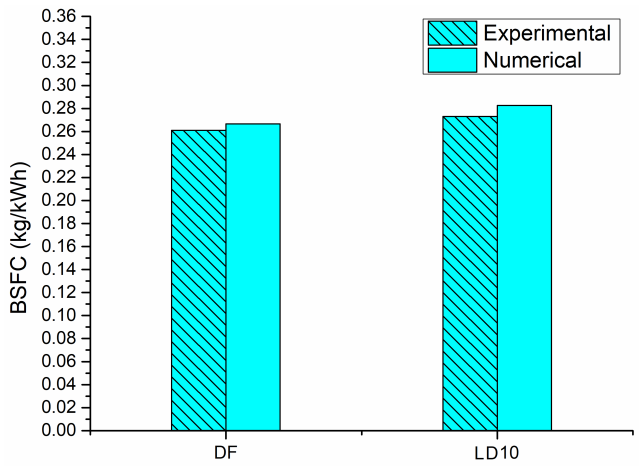

Figure 10. Comparison of BFSC at 2400 rpm and full load between experimental and numerical results.

those from the experiments, and the errors are within 2.1% and 3.5% respectively. It indicates the high precision of the models.

Figure 11 indicates that numerical NO_x emissions of both fuels agree well with experimental data with the bias of 0.2% and 1.6% because NO_x emissions are mainly influenced by combustion temperature in the models, which is determined by the LHV of each fuel and engine conditions.

Engine optimization

Optimization aims to discover the best combination of key operational and geometric parameters of the engine running on LD10. After the optimization, it is anticipated that the diesel engine could still output similar power with LD10 but alleviated emissions. The optimization is carried out at 2400 rpm speed and 100% load at combinations of different

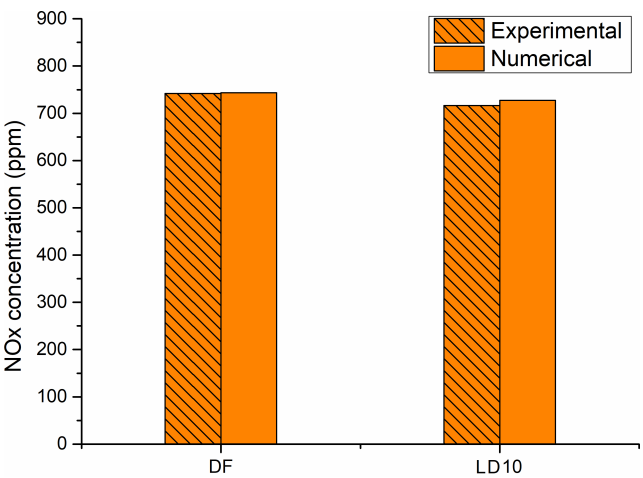

Figure 11. Comparison of NO_x emissions at 2400 rpm and full load between experimental and numerical results.

© 2021 The Authors. *Biofuels, Bioproducts and Biorefining* published by Society of Chemical Industry and John Wiley & Sons, Ltd.

injection pressures, different injection timings, different injection durations, and nozzle diameters.

The fuel injection pressure is a crucial factor affecting fuel spray and combustion. The default setting of the engine is 214 bar. The test injection pressure is thus set to the range from 114 to 514 bar, as shown in Table 5, while the other three parameters are at default values. Figure 12 illustrates the brake power, BSFC, NO_x emissions, and HC emissions of LD10 at 2400 rpm speed and 100% load, where the blue bars are benchmarking data from the experiments and the red line illustrates the referencing experimental data of DF.

Table 5. Parameters for the engine optimization.

Parameter	Default setting	Variable values
Injection pressure (bar)	214	114, 214, 314, 414, 514
Injection timing (°CA)	−15	−18, −15, −12, −9, −6, −3
Injection duration (°CA)	21.1	11.1, 21.1, 31.1, 41.1
Nozzle diameter (mm)	0.17	0.17, 0.37, 0.57, 0.97, 1.17

As illustrated in Fig. 12(a), the brake power decreases with increasing injection pressure. A plausible explanation is that more power is consumed by the fuel pump. In contrast, the BSFC and NO_x emissions both increase with increasing injection pressure, as shown in Fig. 12(b),(c). It means that more fuel is injected at higher injection pressure and thus releases more heat to increase the in-cylinder temperature, which promotes the generation of NO_x emissions. In Fig. 12(d), HC emissions are relatively stable at various injection pressures. Overall, the change of injection pressure has a moderate impact on engine performance.

Injection timing is an important factor associated with the combustion process and thus influences various pollutant emissions. The default setting of the start of injection (SOI) for the engine is −15° CA. The brake power, BSFC, NO_x emissions and HC emissions obtained at the default SOI are the blue bars in (a), (b), (c) and (d) in Fig. 13, respectively. The SOI to be compared in the model are variable from

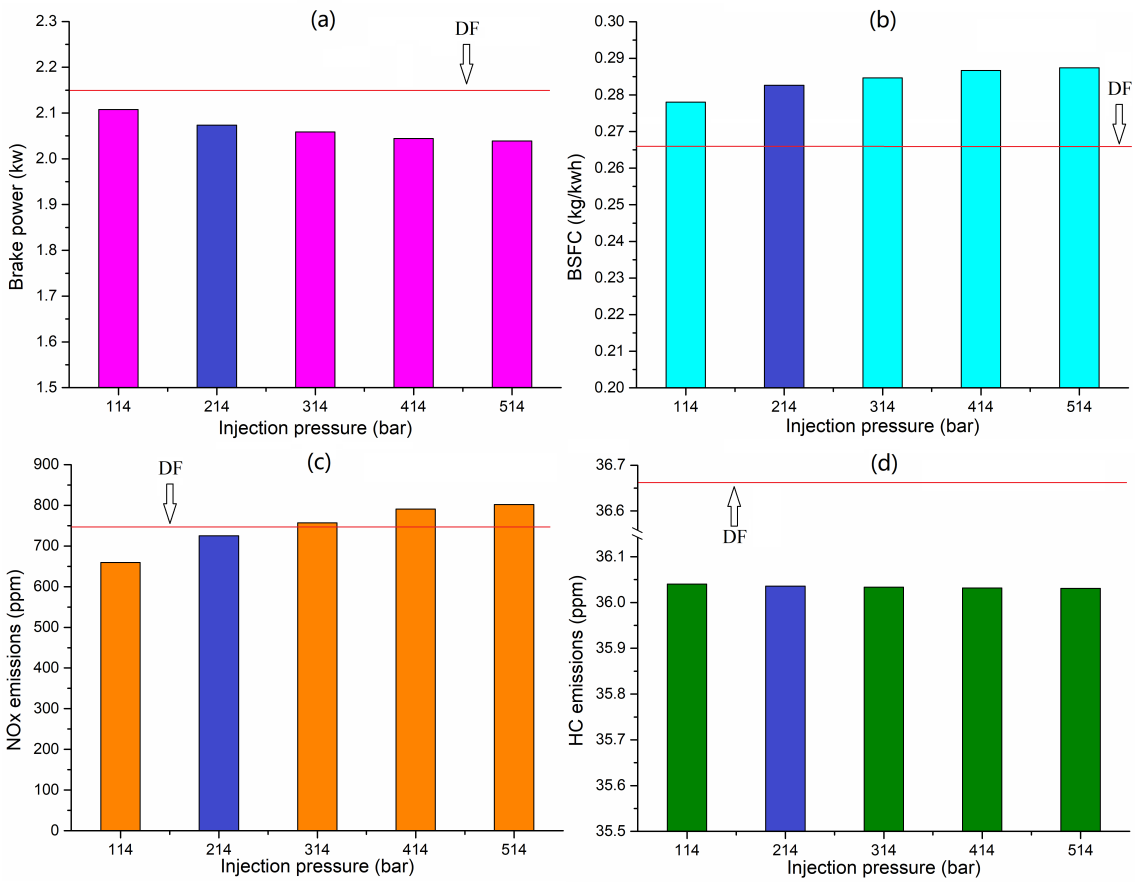

Figure 12. Influence of injection pressure on brake power (a), BSFC (b), NO_x emissions (c) and HC emissions (d).

© 2021 The Authors. *Biofuels, Bioproducts and Biorefining* published by Society of Chemical Industry and John Wiley & Sons, Ltd.

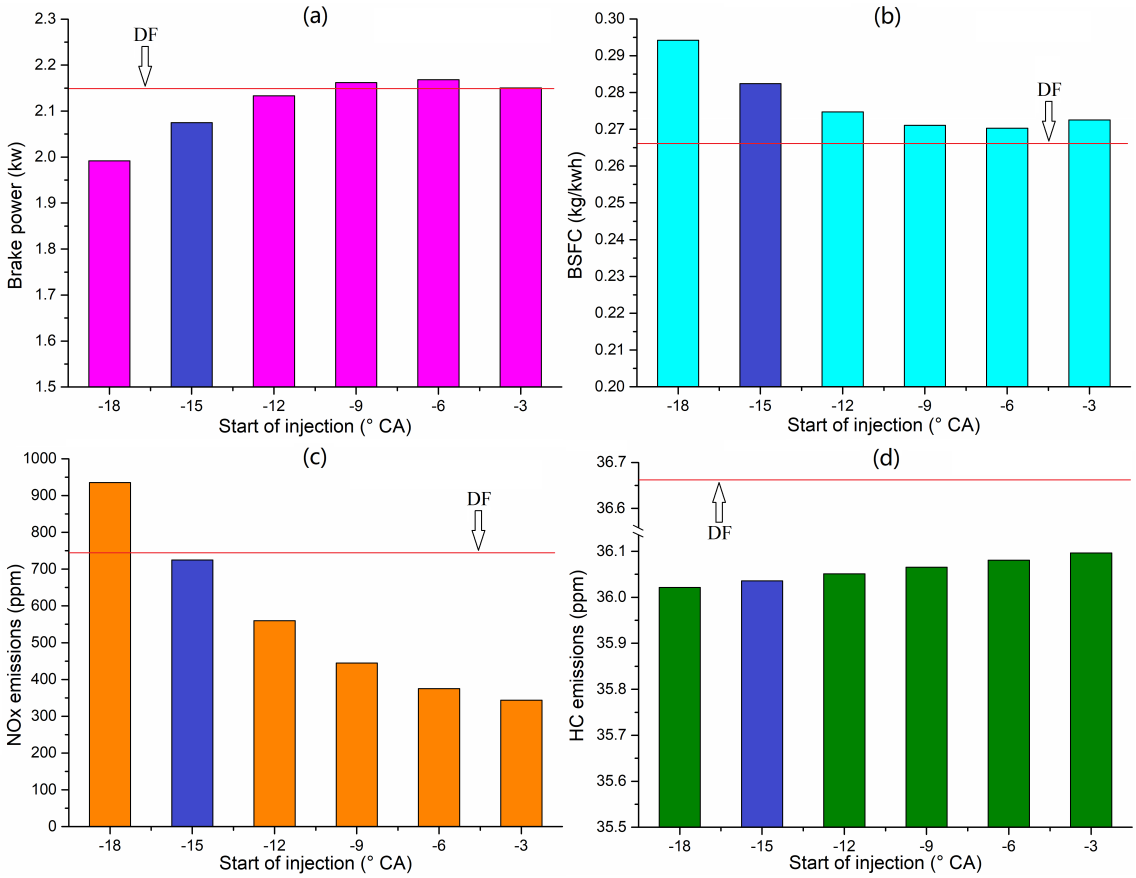

Figure 13. Influence of injection timing on brake power (a), BSFC (b), NO_x emissions (c) and HC emissions (d).

−18° CA to −3° CA, while the other three parameters are all fixed at the default values.

Figure 13(a) shows the brake power increases with retarded SOI until about −6° CA, after which the brake power starts to drop at later SOI. Usually, if the SOI is either too early or too late, it will not benefit to combustion process of the engine. When the injection is retarded and close to the TDC, the ignition delay would be extremely short and the fuel spray would not be developed fully, which results in incomplete combustion and thus reduces the output power. When the SOI is advanced, the ignition delay is extended, which means the injected fuel has more time to mix with air and thus experiences more sufficient combustion. But if SOI is too early, more fuel is burnt in the compression stroke and less fuel is used for combustion during expansion stroke, given that the overall injection duration keeps constant. As a result, less fuel is used to provide power, although the in-cylinder temperature is higher.

Figure 13(b) demonstrates that BSFC has an opposite tendency to brake power. At −6° CA, the lowest BSFC is seen. As less fuel is injected for the combustion during cylinder expansion at advanced SOI, more fuel must be injected to maintain the output power, which increases the fuel consumption. As for significantly retarded SOI, incomplete combustion also leads to more fuel injected for the required output power. With retarded SOI, NO_x emissions decrease but the HC emissions increase, as shown in Fig. 13(c),(d). In general, high NO_x is caused by a higher temperature-activated thermal NO_x formation mechanism whilst SOI is greatly advanced. High HC emissions are produced during the incomplete combustion due to heavily retarded SOI.

Injection duration also plays an important role in determining the fuel consumption and the power output. The default setting of injection duration is 21.1° CA. The brake power, BSFC, NO_x emissions and HC emissions obtained in the default injection duration are the blue bars in (a), (b), (c) and (d) in Fig. 14. The injection duration varies in the range from 11.1° CA to 41.1° CA in the optimization study, whereas the other three parameters are fixed at the default settings.

As illustrated in Fig. 14(a), the brake power of the engine is low at the shortest injection duration, and then gradually increases at longer injection duration. The SOI is fixed at −15° CA, which means that no fuel is injected for combustion in the expansion stroke when the injection duration is 11.1° CA. This is the reason why the output power is significantly

© 2021 The Authors. *Biofuels, Bioproducts and Biorefining* published by Society of Chemical Industry and John Wiley & Sons, Ltd.

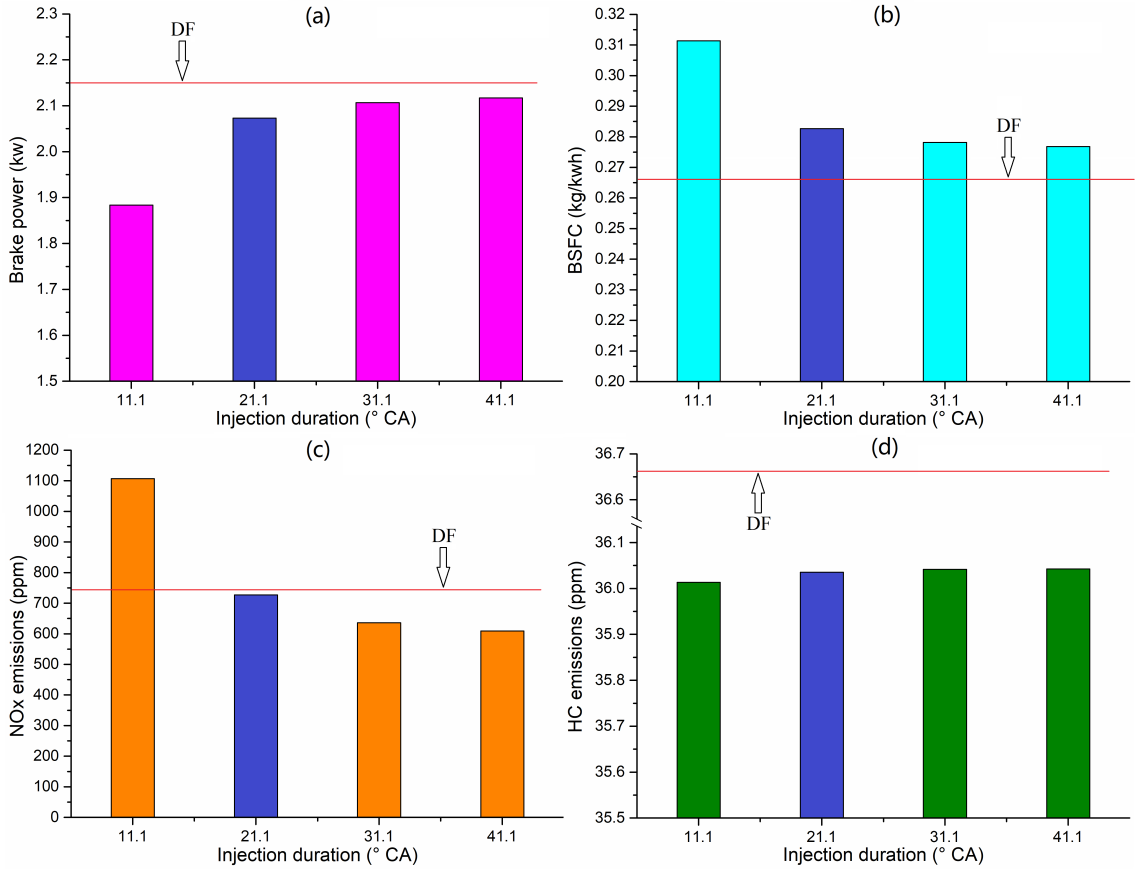

Figure 14. Influence of injection duration on brake power (a), BSFC (b), NO_x emissions (c) and HC emissions (d).

reduced at an injection duration of 11.1° CA. For the other three injection durations, fuel injection happens in both compression and expansion strokes. Generally, longer injection duration means more fuel is burnt to generate more power. To maintain the overall level of power at short injection duration, more fuel has to be injected for combustion in a short period of time to further improve in-cylinder temperature and pressure, which assists NO_x production. It explains the phenomena that NO_x emissions increase when injection duration is shortened, as shown in Fig. 14(c). In Fig. 14(b), it is observed that BSFC is higher when the injection duration is shorter, which is mainly caused by the reduction of output power. Figure 14(d) demonstrates that HC emission increases gradually with extended injection duration, because more fuel is injected at longer injection duration thus leading to incomplete combustion in the cylinder.

The injector orifice is a geometric factor that determines fuel spray morphology and thus influences both combustion and engine power. The default injector orifice of the engine in the experimental study is 0.17 mm. The brake power, BSFC, NO_x emissions and HC emissions obtained using the default orifice are the blue bars in (a), (b), (c) and (d) in Fig. 15, respectively. In the optimization study, the injector orifice is set within the range from 0.17 to 1.17 mm and the other three parameters are set to their default values.

In Fig. 15(a), the brake power increases when the injector orifice diameter is expanded until 0.57 mm. Beyond 0.57 mm, the brake power largely stays constant. With the orifice increasing to 0.57 mm, more fuel is injected and thus releases more heat for power. When the orifice is larger than 0.57 mm, the amount of injected fuel has reached its maximum, and thus cannot further increase brake power. In this way, BSFC is higher when the injector orifice is smaller than 0.57 mm, and remains stable at a larger 0.57 mm orifice, as demonstrated in Fig. 15(b). The NO_x emissions monotonically decrease in Fig. 15(c). The reason is twofold: first, more injected fuel and a larger injector orifice means more heat is absorbed during evaporation, which reduces in-cylinder temperature and thus prohibits formation of NO_x; second, a smaller orifice promotes fuel spray and thus results in more complete combustion, which increases in-cylinder temperature and then benefits NO_x generation.

According to the analysis above, the optimal injection parameters can be confirmed for LD10 at 2400 rpm speed and full load. The optimal injection timing (SOI), injection

© 2021 The Authors. *Biofuels, Bioproducts and Biorefining* published by Society of Chemical Industry and John Wiley & Sons, Ltd.

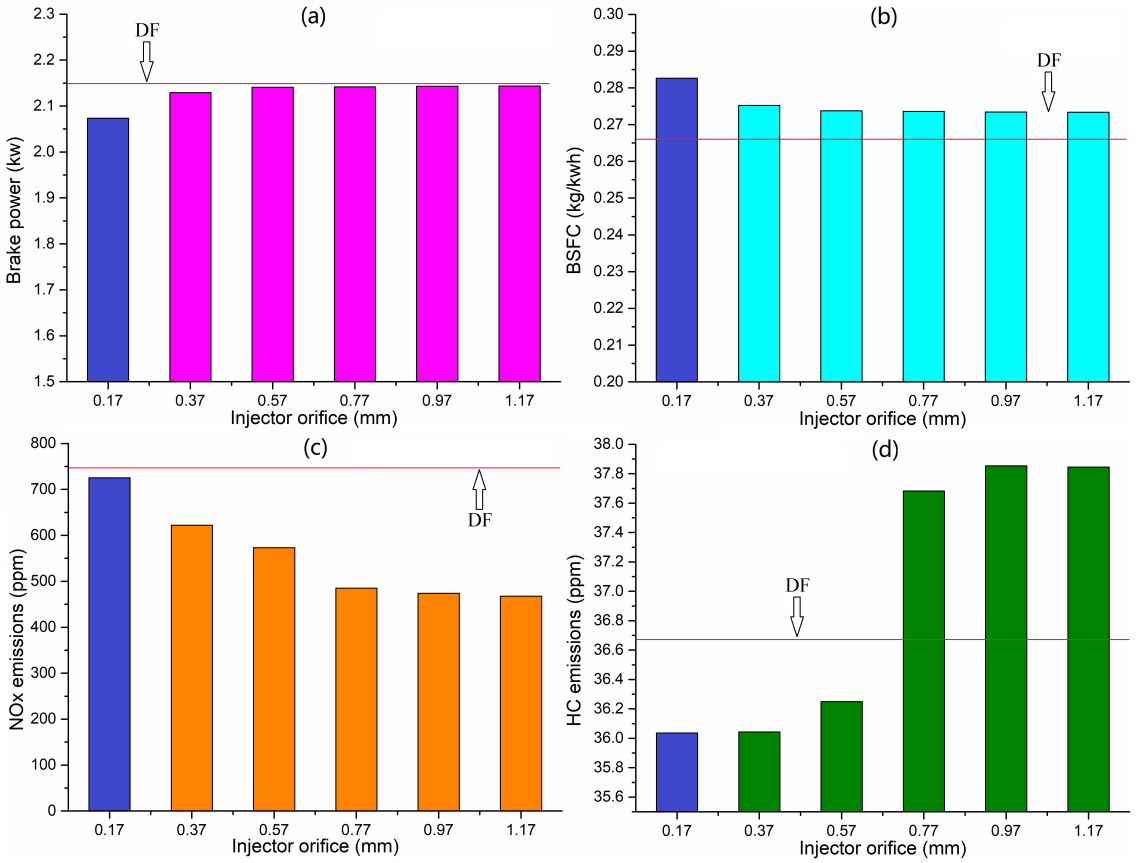

Figure 15. Influence of injector orifice on brake power (a), BSFC (b), NO_x emissions (c) and HC emissions (d).

Table 6. Optimal injection parameters.

Parameter	Injection pressure (bar)	Injection timing (°CA)	Injection duration (°CA)	Injector orifice (mm)
Value	214	–6	41.1	0.37

duration and injector orifice are listed in Table 6. The injection pressure stays the same as the default engine setting, as it cannot change the engine performance significantly, compared with other injection parameters.

The optimal brake power, BSFC, NO_x emissions and HC emissions are therefore obtained through the optimization study on the validated model, which are shown in Fig. 16.

According to Fig. 16, the optimized engine model using LD10 has very similar BSFC and HC emissions as the benchmarking model using DF as a fuel. Meanwhile, the brake power of the optimized LD10 model is improved by about 2.3%, whereas the NO_x emissions are reduced by about 58%. After the optimization, the testing engine is therefore expected to significantly reduce pollutant emissions with no negative impact on power output and fuel consumption when using LD10, compared with that burning DF at the same engine speed and load.

To further reduce the life-cycle carbon emissions, the ratio of 2M4PP in the blend is increased to 50% in the simulation to predict the engine performance and emissions. Apart from expected major carbon emission reduction, it is found that NO_x and HC are deducted by 13.9% and 8.8% respectively compared with those of DF. Due to the further decreasing heating value of LD50 compared to that of diesel, the brake power is reduced by 19.7% and the BSFC is increased by 6.7%. It indicates that although the life-cycle carbon emissions could be reduced further with a higher content of monomeric aromatic oxygenates in the diesel blend, engine power loss and increasing fuel consumption would create new problems in implementation. Due to the common redundancy of overall engine power and fuel tank capacity on board ships, LD50 may be still appliable. An in-depth investigation based on a case ship is needed before any conclusion can be reached. Engine durability and lubricant oil

© 2021 The Authors. *Biofuels, Bioproducts and Biorefining* published by Society of Chemical Industry and John Wiley & Sons, Ltd.

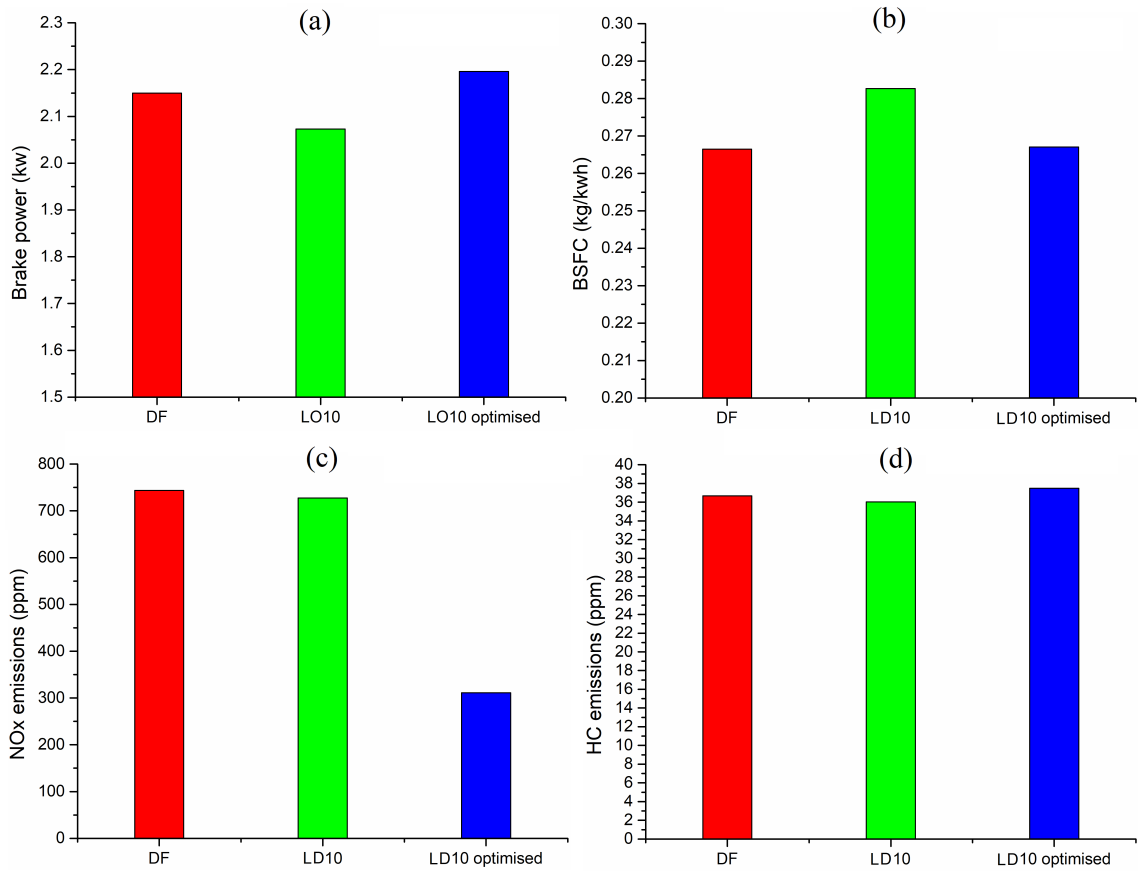

Figure 16. Comparison among DF, LD10 with default engine parameters and LD10 with the optimal engine parameters.

compatibility are the other two issues worth to be scrutinized. In summary, there could be a trade-off between emission abatement and engine performance in the real marine application of the new lignin derived biofuel.

Conclusions

In this paper, the performance of 2M4PP blended with DF (LD10) is investigated by experiments on a diesel engine. The numerical Ricardo WAVE models of the engine fueled with DF and LD10 are developed and validated using the experimental data of in-cylinder pressure, brake power, BSFC and NO_x emissions. Optimal engine performance and emissions are identified for this model with a detailed analysis of the influences of injection parameters. It is concluded that:

- The in-cylinder pressure profile of the LD10-fueled diesel engine is very close to that of the DF-fueled engine, but the BSFC of it is higher due to the greater density of LD10.
- The engine using LD10 emits lower CO and NO_x than the same model using DF, due to the oxygen content in LD10, which promotes oxidization of CO and reduces combustion temperature.
- Fuel injection pressure has no significant impact on engine performance when LD10 is used as a fuel.
- A retarded SOI and increasing injection duration both benefits brake power and BSFC, with the best performance achieved at −6° (SOI) and 31.1° (injection duration), which also assists in reducing NO_x emissions at a small penalty of a slight HC emission increase.
- A moderately enlarged injector orifice significantly reduces NO_x emissions and slightly increases the HC emission. When the orifice diameter exceeds 0.57 mm, the HC emission increases dramatically, and further NOx emission reduction is achieved.
- The optimized injection parameters for the engine burning LD10 at 2400 rpm and full load are 214 bar (injection pressure), 6° (injection timing), 41.4° (injection duration) and 0.37 mm (injector orifice). Under these settings, the engine could obtain improved brake power and reduced NO_x emissions without comparable impacts on fuel consumption and HC emissions, compared with using standard DF.

The switch from fossil to renewable fuels in the shipping industry is crucial to reduce the emissions of GHGs and other pollutants such as NO_x and SO_2. For the maritime sector, liquid

© 2021 The Authors. *Biofuels, Bioproducts and Biorefining* published by Society of Chemical Industry and John Wiley & Sons, Ltd.

renewable drop-in fuels are viewed as a very viable option for the mid-term to long-term (30–40 years). Investigating monomeric aromatic oxygenates (such as 2M4PP) therefore represents the first step towards understanding the combustion behavior of more complex bio-oil mixtures that might arise in the future from 2G biorefineries (mixtures of lignin monomers and lignin oligomers).

Acknowledgements

The authors appreciate the UK Engineering and Physical Sciences Research Council (EPSRC) for financial support through research grants EP/S00193X/1 and EP/S00193X/2. This work was also performed under the framework of Chemelot InSciTe and is supported by financial contributions from the European Interreg V Flanders, the European Regional Development Fund (ERDF) within the framework of OP-Zuid, the province of Brabant and Limburg and the Dutch Ministry of the Economy.

References

1. Smith T, Jalkanen J, Anderson B, *et al*. Reduction of GHG emissions from ships: third IMO GHG Study 2014–Final Report, IMO. (2014).
2. Organisation IM. Nitrogen Oxides (NOx) – Regulation 13. (2018) http://www.imo.org/en/OurWork/Environment/PollutionPrevention/AirPollution/Pages/Nitrogen-oxides-(NOx)-%E2%80%93-Regulation-13.aspx.
3. Organisation IM. Sulphur Oxides (SOx) and Particulate Matter (PM) – Regulation 14. (2018).
4. Shen X, Shi J, Cao X, Zhanga X, Zhanga W, Wu H *et al*., Real-world exhaust emissions and fuel consumption for diesel vehicles fueled by waste cooking oil biodiesel blends. *Atmos Environ* **191**:249–257 (2018).
5. Jeon J and Park S, Effects of pilot injection strategies on the flame temperature and soot distributions in an optical CI engine fueled with biodiesel and conventional diesel. *Appl Energy* **160**:581–591 (2015).
6. Özener O, Yüksek L, Ergenç AT and Özkan M, Effects of soybean biodiesel on a DI diesel engine performance, emission and combustion characteristics. *Fuel* **115**:875–883 (2014).
7. Nabi MN, Zare A, Hossain FM, Ristovskib ZD and Brown RJ, Reductions in diesel emissions including PM and PN emissions with diesel-biodiesel blends. *J Clean Prod* **166**:860–868 (2017).
8. Zhou L, Boot M and Johansson BJF, Comparison of emissions and performance between saturated cyclic oxygenates and aromatics in a heavy-duty diesel engine. *Fuel* **113**:239–247 (2013).
9. Ľudmila H, Michal J, Andrea Š and Aleš H, Lignin, potential products and their market value. *Wood Res* **60**:973–986 (2015).
10. Michelin M, Ruíz HA, Silva DP, Ruzene DS, Teixeira JA and Polizeli MLTM, Cellulose from lignocellulosic waste. *Polysaccharides: Bioactivity and Biotechnology*. Springer International Publishing, 1, Switzerland, pp. 475–511 (2015).
11. Sun X, Zhao X, Zu Y, Li W and Ge Y, Preparing, characterizing, and evaluating ammoniated lignin diesel from papermaking black liquor. *Energy Fuels* **28**:3957–3963 (2014).
12. Boot MD. Liquid fuel composition and the use thereof. Google Patents. WO2008088212 (2016).
13. Tian M, Van Haaren R, Reijnders J and Boot M, Lignin derivatives as potential octane boosters. *SAE Int J Fuels Lubr.* **8**:415–422 (2015).
14. Zhou L, Boot M, Johansson B and Reijnders JJE, Performance of lignin derived aromatic oxygenates in a heavy-duty diesel engine. *Fuel* **115**:469–478 (2014).
15. Kumar BR, Saravanan S, Kumar RN, Nishanth B, Rana D and Nagendran A, Effect of lignin-derived cyclohexanol on combustion, performance and emissions of a direct-injection agricultural diesel engine under naturally aspirated and exhaust gas recirculation (EGR) modes. *Fuel* **181**:630–642 (2016).
16. Demirbas A and Demirbas MF, Importance of algae oil as a source of biodiesel. *Energy Convers Manage* **52**:163–170 (2011).
17. Renders T, Van den Bosch S, Koelewijn S-F, Schutyser W and Sels BF, Lignin-first biomass fractionation: the advent of active stabilisation strategies. *Energy Environ Sci* **10**:1551–1557 (2017).
18. Shuai L, Amiri MT, Questell-Santiago YM, Héroguel F, Li Y, Kim H *et al*., Formaldehyde stabilization facilitates lignin monomer production during biomass depolymerization. *Science* **354**:329–333 (2016).
19. McCormick RL, Baldwin RM, Arbogast S *et al*., Biofuels from Lignocellulosic Biomass: Innovations beyond Bioethanol Biomass pyrolysis oils. Wiley-VCH Verlag GmbH & Co. KGaA, **40**:189–207 (2016).
20. Abu-Omar MM, Barta K, Beckham GT, Luterbacher JS, Ralph J, Rinaldi R *et al*., Guidelines for performing lignin-first biorefining. *Energy Environ Sci* **14**:262–292 (2021).
21. Kouris PD, Huang X, Boot MD, *et al*. Drop-in diesel biofuels from lignin monomers: from production to combustion. 6th TMFB Conference Tailor-Made Fuels: From production to propulsion Aachen (2018).
22. Ferrini P and Rinaldi R, Catalytic biorefining of plant biomass to non-pyrolytic lignin bio-oil and carbohydrates through hydrogen transfer reactions. *Angew Chem Int Ed Engl* **126**:8778–8783 (2014).
23. Huang X, Korányi TI, Boot MD and Hensen EJM, Ethanol as capping agent and formaldehyde scavenger for efficient depolymerization of lignin to aromatics. *Green Chem* **17**:4941–4950 (2015).
24. Zakzeski J, Jongerius AL, Bruijnincx PC and Weckhuysen BM, Catalytic lignin valorization process for the production of aromatic chemicals and hydrogen. *ChemSusChem* **5**:1602–1609 (2012).
25. Van den Bosch S, Schutyser W, Vanholme R, Driessen T, Koelewijn S-F and Renders T, Reductive lignocellulose fractionation into soluble lignin-derived phenolic monomers and dimers and processable carbohydrate pulps. *Energy Environ Sci* **8**:1748–1763 (2015).
26. Huang X, Zhu J, Korányi TI, Boot MD and Hensen EJM, Effective release of lignin fragments from lignocellulose by Lewis acid metal triflates in the lignin-first approach. *ChemSusChem* **9**:3262–3267 (2016).
27. Van den Bosch S, Schutyser W, Koelewijn S-F, Renders T, Courtinb CM and Sels BF, Tuning the lignin oil OH-content with Ru and Pd catalysts during lignin hydrogenolysis on birch wood. *Chem Commun* **51**:13158–13161 (2015).
28. Huang X, Ouyang X, Hendriks BM, Gonzalez OMM, Zhu J, Korányi TI *et al*., Selective production of mono-aromatics from lignocellulose over Pd/C catalyst: the influence of acid co-catalysts. *Faraday Discuss* **202**:141–156 (2017).

© 2021 The Authors. *Biofuels, Bioproducts and Biorefining* published by Society of Chemical Industry and John Wiley & Sons, Ltd.

29. Gowdagiri S, Wang W and Oehlschlaeger MA, A shock tube ignition delay study of conventional diesel fuel and hydroprocessed renewable diesel fuel from algal oil. *Fuel* **128**:21–29 (2014).
30. McCormick RL, Ratcliff MA, Christensen E, Fouts L, Luecke J, Chupka GM *et al*., Properties of oxygenates found in upgraded biomass pyrolysis oil as components of spark and compression ignition engine fuels. *Fuel* **29**:2453–2461 (2015).
31. PubChem. 2-Methoxy-4-propylphenol (2019). https://pubchem.ncbi.nlm.nih.gov/compound/Dihydroeugenol .
32. Boot M, *Biofuels from Lignocellulosic Biomass: Innovations beyond Bioethanol*. John Wiley & Sons, Germany (2016).
33. Habib Z, Parthasarathy R and Gollahalli S, Performance and emission characteristics of biofuel in a small-scale gas turbine engine. *Appl Energy* **87**:1701–1709 (2010).
34. Lefebvre AH, *Gas Turbine Combustion*. CRC press, US (1998).

Zhichao Zhang

Zhichao Zhang, born in August 1988, is a lecturer at Northumbria University. He graduated from the Civil Aviation University of China in 2012 and Beihang University in 2015 with his bachelor and master degrees. He was awarded the Doctoral Training Award of the SAgE Faculty from Newcastle University, and obtained his PhD in 2019. He completed his postdoc research in Delft University of Technology in Netherlands from 2019 to 2020. Zhichao has produced six papers on applied energy and fuel, two conference papers, and one patent. His previous research work was on the NSFC project 'Fundamental study of Quasi-hydrous Ethanol and Bio-jet Fuel Blends and their Influence on the Characteristics of Blow Off and Smoking Boundary', the BNSF project 'Establishment of Particulate Emission Index on GDI Engines', and the EPSRC funded project 'Investigation Into Fuel Pre-treatments For Combustion Improvement on a Compression Ignition Engine.' He is currently researching the problem of hydrogen diffusion in turbine blades for the utilization of hydrogen fuel.

Georgios D. Kouris

Georgios Kouris received a bachelor's degree in Naval Architecture from the University of West Attica. After finishing his undergraduate studies, he was employed for 1 year as a junior naval architect in a technical company, in which his main responsibility was the 3D geometric modeling of ships for damage stability. From 2017 he studied at Newcastle University for his MSc marine engineering. During that period, his conducted research on fuel consumption and the emissions of a four-stroke marine diesel engine, operated with a biofuel based on lignin (crude lignin oil). In 2018 he joined Alpha Marine Consulting PC.

Panos D. Kouris

Panos Kouris holds an MSc in chemical engineering and is a researcher in the inorganic materials and catalysis group at Eindhoven University of Technology, finalizing his PhD research in the field of thermocatalytic biomass conversion. Since 2017 he has been the co-founder and Chief Technology Officer of Vertoro, the commercialization vehicle of a proprietary biomass-to-lignin oil technology enterprise.

Emiel J. M. Hensen

Emiel Hensen is a professor of inorganic materials and catalysis at Eindhoven University of Technology. His research focuses on the fundamental and applied aspects of catalyzed reactions relevant to clean and sustainable processes for the production of fuels and chemicals with the aim of identifying active sites and understanding reaction mechanisms. Applications are directed towards the improvement of current industrial chemical processes and novel processes based on renewable feedstock, such as biomass. Catalytic target reactions are methane activation, Fischer–Tropsch catalysis, environmental catalysis, zeolite catalysis, conversion of biogenic molecules such as sugars and lignin, metal-support cooperativity in selective oxidation, CO_2 reduction and photocatalysis.

Michael D. Boot

Michael Boot is a fellow in the inorganic materials and catalysis group at Eindhoven University of Technology and co-founder and CEO at Vertoro. His applied research on, and valorization, of biomass focuses on thermal (acid) solvolysis of lignin and lignocellulose to lignin-rich oils, which can be further (catalytically) upgraded to fuels, chemicals, and materials.

Dawei Wu

Dawei Wu is a UK EPSRC fellow and a senior lecturer in mechanical engineering at the University of Birmingham. His expertise is in the decarbonization of combustion engines using e-fuels (e.g., hydrogen, ammonia, and methane) and biofuels. He aims to develop novel low-carbon fuel-fired propulsion and power systems, especially for marine applications.

© 2021 The Authors. *Biofuels, Bioproducts and Biorefining* published by Society of Chemical Industry and John Wiley & Sons, Ltd.